

Article

## Heterogeneous Nucleation Rate of Calcium Carbonate Derived from Induction Period

Wen-Chen Chien, Chuang-Chung Lee, and Clifford Y. Tai

*Ind. Eng. Chem. Res.*, **2007**, 46 (20), 6435-6441 • DOI: 10.1021/ie061416+

Downloaded from <http://pubs.acs.org> on November 25, 2008

### More About This Article

Additional resources and features associated with this article are available within the HTML version:

- Supporting Information
- Access to high resolution figures
- Links to articles and content related to this article
- Copyright permission to reproduce figures and/or text from this article

[View the Full Text HTML](#)



**ACS Publications**  
High quality. High impact.

# Heterogeneous Nucleation Rate of Calcium Carbonate Derived from Induction Period

Wen-Chen Chien,<sup>†</sup> Chuang-Chung Lee,<sup>‡</sup> and Clifford Y. Tai<sup>\*,‡</sup>

Department of Chemical Engineering, Mingchi University of Technology, 84 Gunjuan Road, Taishan, Taipei Hsien 243, Taiwan, and Department of Chemical Engineering, National Taiwan University, Taipei, Taiwan

The induction period,  $t_{\text{ind}}$ , in the process of heterogeneous nucleation of  $\text{CaCO}_3$  in aqueous  $\text{CaCl}_2\text{--Na}_2\text{CO}_3$  solution was investigated. The  $t_{\text{ind}}$  was measured by applying the conductivity method. Diatomaceous earth and zirconium oxide were used as foreign particles to induce heterogeneous nucleation. The experimental results showed that  $t_{\text{ind}}$  decreased with an increase in supersaturation and the solid concentration of foreign particles. The solid concentration of foreign particles had a great influence on  $t_{\text{ind}}$  at low supersaturations; however, the effect of foreign particles was negligible at high supersaturations. A novel model of  $t_{\text{ind}}$  for the heterogeneous nucleation was derived by using the Michaelis–Menten equation. In this model, the heterogeneous nucleation rate,  $J_{\text{h}}$ , was considered to be the sum of the bulk nucleation rate,  $J_{\text{b}}$ , and the particle-induced nucleation rate,  $J_{\text{p}}$ , where  $J_{\text{b}}$  and  $J_{\text{p}}$  were contributed from the bulk of solution and the surface of added foreign particles, respectively. The results showed that  $J_{\text{h}}$  could be expressed simply as a function of the supersaturation and the solid concentration of foreign particles. The affinity,  $K_{\text{M}}$ , between calcium carbonate and foreign particles obtained from the diatomaceous earth was greater than that obtained from the zirconium oxide. A comparison between the calculated and experimental results showed that the Michaelis–Menten equation was satisfactory to describe the experimental data of  $t_{\text{ind}}$  and to derive the nucleation rate for the heterogeneous nucleation of calcium carbonate.

## Introduction

The crystallization process from a supersaturated solution involves nucleation and crystal growth. The rate of nucleation plays an important role in controlling the final particle size distribution. From the statistical concept of nucleation, the mean time of critical nucleus formation is equal to  $t_{\text{ind}} = 1/J$ , where  $t_{\text{ind}}$  is the induction period, and  $J$  is the nucleation rate.<sup>1,2</sup> Since the induction period is closely related to the nucleation rate and is easy to measure in a crystallization experiment, many efforts have been devoted to seek a theoretical expression that can be used to calculate the induction period and thus estimate the nucleation rate and interpret the experimental results of the nucleation process.

The induction period is defined as the time that elapses between the creation of supersaturation and the formation of critical nuclei. Many methods have been applied for the determination of the induction period, including the conductivity method,<sup>3,4</sup> the intensity of transmitted or scattered light method,<sup>5–7</sup> the heat released method,<sup>8,9</sup> the activity of precipitated ions method, and the pH method.<sup>10,11</sup> It was found that the induction period was affected greatly by several important factors such as supersaturation, temperature, pH, agitation speed, and the presence of impurity, seed, or foreign particle.<sup>3,4,11–13</sup> The induction period decreases with an increase in supersaturation, temperature, and agitation speed, but it increases with the presence of an impurity. The presence of seed or foreign particle also decreases the induction period.

Söhnel and Mullin plotted  $\log t_{\text{ind}}$  versus  $(\log S_{\text{a}})^{-2}$ , where  $S_{\text{a}}$  is supersaturation, for the precipitation of  $\text{CaCO}_3$  over a wide

range of supersaturations.<sup>14</sup> The experimental data obtained can be fitted by two straight lines of different slopes, which indicated that there may exist two different nucleation mechanisms, that is, heterogeneous nucleation at low supersaturation and homogeneous nucleation at high supersaturation. van der Leeden et al. analyzed the induction period data obtained from both unseeded and seeded precipitation of  $\text{BaSO}_4$  and  $\text{CaCO}_3$ . The analysis revealed that the nucleation mechanism for both systems is heterogeneous primary nucleation.<sup>10</sup> Recently, Nomura et al. proposed a modified cell model to describe the process of simultaneous homogeneous and heterogeneous nucleation. The model enables us to predict the relative importance of homogeneous and heterogeneous nucleation as a function of the operating conditions, including concentration of monomers and the concentration and size of particles.<sup>15</sup> Liu derived a new kinetic model for the heterogeneous nucleation in which the effects of foreign particles on the nucleation barrier, the chain reaction process, and the transport of structure units are taken into account.<sup>16</sup> Although the present expressions enable us to predict the heterogeneous nucleation rate, the reported expressions were complex, and some parameters were difficult to determine experimentally.

In the present paper, the formation of critical nuclei by heterogeneous nucleation is assumed because of the absorption–desorption mechanism between the calcium carbonate and foreign particles. A simple correlation of the heterogeneous nucleation rate and the induction period was obtained and expressed by a function of the supersaturation and the solid concentration of foreign particles. The effect of particle concentration on the induction period was investigated. In addition, the affinity between calcium carbonate and different kinds of foreign particles was also studied.

\* Author to whom correspondence should be addressed. Tel: 886-2-23620832. Fax: 886-2-23623040. E-mail: cytai@ntu.edu.tw.

<sup>†</sup> Mingchi University of Technology.

<sup>‡</sup> National Taiwan University.

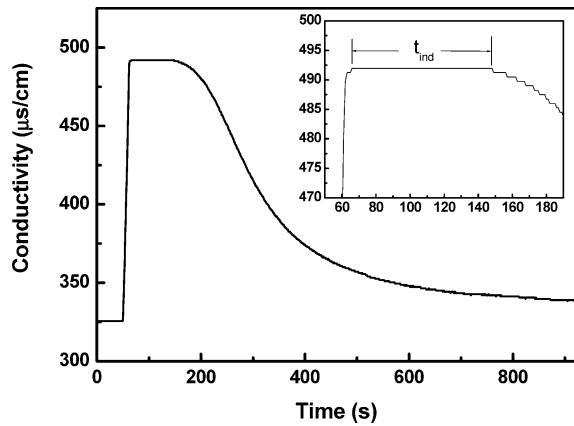


**Figure 1.** A typical desupersaturation curve for the mixing of 0.0020 M  $\text{CaCl}_2$  and  $\text{Na}_2\text{CO}_3$  solution with 2 mg of diatomaceous earth as the foreign particle at 298 K. The induction period can be determined when that portion of the desupersaturation curve is enlarged, as shown in the upper right corner.

**Table 1. Induction Period of  $\text{CaCl}_2$ – $\text{Na}_2\text{CO}_3$  Solution at Various Supersaturations in the Presence of Diatomaceous Earth as the Foreign Particle**

W (mg)	[FP] (no./ $\text{cm}^3$ )	$t_{\text{ind}}$ (s)				
		$S_a = 4.59$	$S_a = 5.49$	$S_a = 5.85$	$S_a = 6.41$	$S_a = 6.90$
0	0	287	182	132	85	44
2	224	218	148	102	68	38
3	335	200	136	92	65	36
5	559	186	120	80	54	32
8	894	152	105	70	48	32
11	1230	138	100	65	48	28
15	1677	130	90	60	44	28

## Theory

The time interval between the onset of supersaturation and the formation of a cluster of detectable size is defined as the induction period,  $t_{\text{ind}}$ . Generally, the nucleation rate can be expressed by the induction period as follows:<sup>1,2</sup>

$$J_h = \frac{1}{t_{\text{ind}}|_{[\text{FP}] \neq 0}} \quad (1)$$

where  $J_h$  and  $t_{\text{ind}}|_{[\text{FP}] \neq 0}$  are the heterogeneous nucleation rate and the induction period in the presence of foreign particles, respectively. [FP] is the concentration of added foreign particles. The total nucleation rate  $J_h$  is assumed to be the sum of the nucleation rate that occurred in the bulk of solution,  $J_b$ , and originated from the surface of added foreign particles,  $J_p$ . Thus

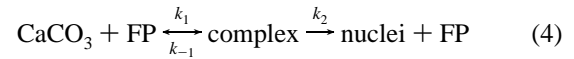
$$J_h = J_b + J_p \quad (2)$$

where  $J_b$  can be estimated by the reciprocal of the induction period without adding foreign particles,  $t_{\text{ind}}|_{[\text{FP}] = 0}$ :

$$J_b = \frac{1}{t_{\text{ind}}|_{[\text{FP}] = 0}} \quad (3)$$

On the other hand, the relationship between  $J_p$  and [FP] is discussed as follows. A novel mechanism for the formation of critical nuclei by heterogeneous nucleation, which is similar to the Michaelis–Menten equation for enzyme kinetics, is assumed, in which the nuclei are produced from the surface of foreign particles.<sup>17</sup> First, the calcium carbonate cluster adsorbed

onto added foreign particles to form the  $\text{CaCO}_3$ –FP complex, and then the calcium carbonate cluster on the complex continues to grow by the adsorption–desorption mechanism. Once the size of the calcium carbonate cluster on the complex is greater than the critical size, the complex is converted into the nuclei and the nuclei break away from the foreign particles. The mechanism can be expressed by the following scheme:



where  $k_1$  and  $k_{-1}$  are the adsorption and desorption rate constants, respectively, and  $k_2$  is the rate constant for the decomposition reaction of the complex. According to this mechanism, the nucleation rate  $J_p$  can be expressed as

$$J_p = \frac{d[\text{nuclei}]}{dt} = k_2[\text{complex}] \quad (5)$$

where [nuclei] and [complex] are the concentrations of the nuclei and the complex, respectively. Here, the pseudo-steady-state assumption is postulated. Thus,

$$\frac{d[\text{complex}]}{dt} = 0 \quad (6)$$

The pseudo-steady-state assumption is quite reasonable since the rate of adsorption is much faster than the desorption and decomposition rates of the complex. It means that the production and consumption rates of the complex are equal during the nucleation stage.

By equalizing the two rates we have

$$k_1[\text{CaCO}_3][\text{FP}] = (k_{-1} + k_2)[\text{complex}] \quad (7)$$

where  $[\text{CaCO}_3]$  is the concentration of free calcium carbonate in the bulk solution. Moreover, the total concentration of calcium carbonate,  $[\text{CaCO}_3]_T$ , is equal to the sum of the free calcium carbonates in the bulk solution and those adsorbed on the surface of foreign particles to form the complex, that is,

$$[\text{CaCO}_3]_T = [\text{CaCO}_3] + [\text{complex}] \quad (8)$$

Substituting eq 8 into eq 7 gives

$$\frac{([\text{CaCO}_3]_T - [\text{complex}])[\text{FP}]}{[\text{complex}]} = \frac{k_{-1} + k_2}{k_1} \quad (9)$$

If we let  $K_M = (k_{-1} + k_2)/k_1$ , eq 9 may be written as

$$[\text{complex}] = \frac{[\text{CaCO}_3]_T[\text{FP}]}{K_M + [\text{FP}]} \quad (10)$$

A low value of  $K_M$  indicates a strong affinity between the calcium carbonate cluster and the foreign particles. Combining eqs 5 and 10, the nucleation rate caused by the effect of foreign particles can be expressed as

$$J_p = \frac{k_2[\text{CaCO}_3]_T[\text{FP}]}{K_M + [\text{FP}]} \quad (11)$$

$J_p$  has a maximum value,  $J_{p,\text{max}}$ , when  $K_M \rightarrow 0$ , that is, all of the calcium carbonate cluster is adsorbed onto foreign particles to form the complex. Therefore,  $J_{p,\text{max}}$  can be written as

$$J_{p,\text{max}} = k_2[\text{CaCO}_3]_T \quad (12)$$

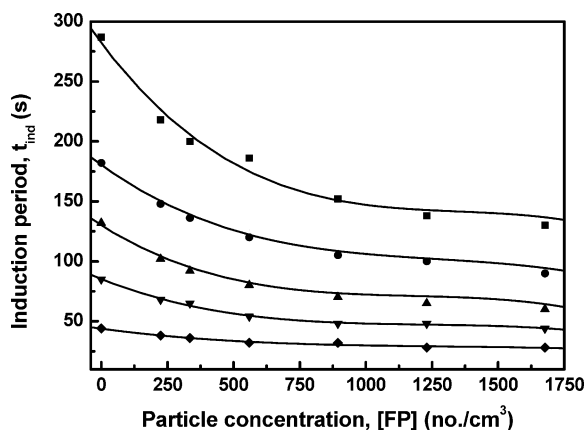


**Figure 2.** Induction period as a function of the concentration of foreign particles at five different levels of supersaturation: (■)  $S_a = 4.59$ ; (●)  $S_a = 5.49$ ; (▲)  $S_a = 5.85$ ; (▼)  $S_a = 6.41$ ; (◆)  $S_a = 6.90$ .

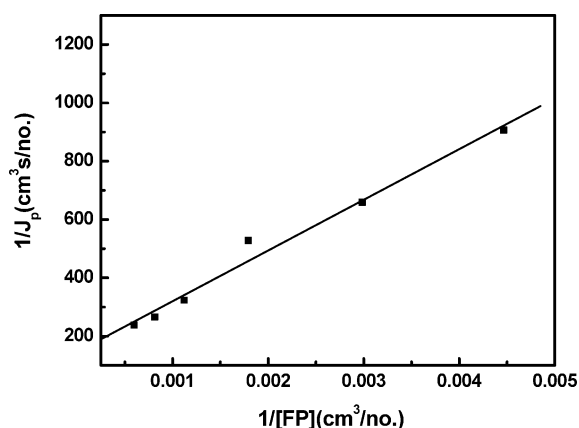


**Figure 3.** Plot of  $1/J_p$  versus  $1/[FP]$  for the foreign particles of diatomaceous earth at  $S_a = 4.59$ .

Substituting eq 11 into eq 12, we have

$$J_p = J_{p,\max} \frac{[FP]}{K_M + [FP]} \quad (13)$$

According to eq 13, the physical meaning of  $K_M$  is the affinity between the calcium carbonate cluster and the foreign particles. The values of  $K_M$  and  $J_{p,\max}$  can be obtained by using the method of a double-reciprocal plot:<sup>17</sup>

$$\frac{1}{J_p} = \frac{K_M}{J_{p,\max}} \frac{1}{[FP]} + \frac{1}{J_{p,\max}} \quad (14)$$

A plot of  $1/J_p$  versus  $1/[FP]$ , in accordance with eq 14, gives a straight line. The slope and intercept of the straight line should allow us to calculate the values of  $K_M/J_{p,\max}$  and  $1/J_{p,\max}$ . Once the value of  $K_M$  and  $J_{p,\max}$  are obtained, the  $J_p$  values at different values of  $[FP]$  can be calculated from eq 13. Additionally,  $J_b$  can be estimated from the experimental data of  $t_{\text{ind}}|_{[FP]=0}$  by using eq 3. Further, we assume that the value of  $J_b$  is not influenced by the presence of added foreign particles. According to eqs 1 and 2, the value of the induction period in the heterogeneous nucleation,  $t_{\text{ind}}|_{[FP] \neq 0}$  can be calculated by

$$t_{\text{ind}}|_{[FP] \neq 0} = \frac{1}{J_b + J_p} \quad (15)$$

## Experimental

The experimental apparatus, which consists mainly of three parts (i.e., a reagent feeding system, a crystallizer with tem-

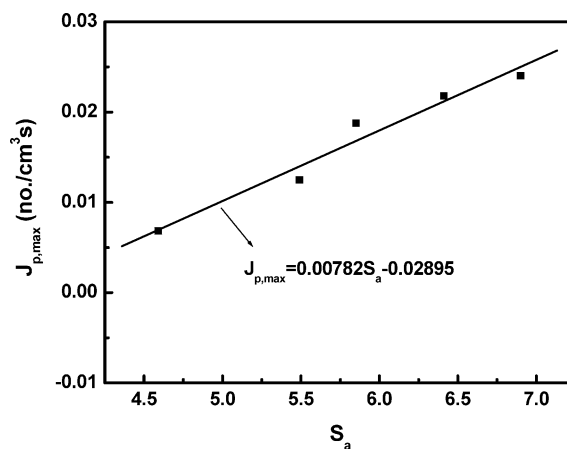


**Figure 4.**  $J_{p,\max}$  as a linear function of  $S_a$  for diatomaceous earth as the foreign particle: (■) calculated points ( $J_{p,\max}$ ,  $S_a$ ).

**Table 2.** Induction Period of  $\text{CaCl}_2\text{-Na}_2\text{CO}_3$  Solution at Various Supersaturations in the Presence of Zirconium Oxide as the Foreign Particle

W (mg)	[FP] (no./cm <sup>3</sup> )	$t_{\text{ind}}$ (s)				
		$S_a = 4.59$	$S_a = 5.49$	$S_a = 5.85$	$S_a = 6.41$	$S_a = 6.90$
0	0	287	182	132	85	44
2	1326	254	166	115	74	41
3	1989	245	160	110	68	38
5	3315	225	148	100	62	36
8	5304	200	136	90	60	36
11	7293	190	128	82	52	34
15	9945	180	120	76	52	34

perature control, and a data acquisition system), has been illustrated in a previous study.<sup>18</sup> The data acquisition system with a high-speed analog/digital board was installed in the computer, and its data sampling speed could be up to 1 MHz. The desupersaturation curve of a solution, which is a plot of conductivity versus time, was obtained by using this data acquisition system, and any portion of the curve could be enlarged to indicate a very small change in conductivity. Chemicals of guaranteed-grade calcium carbonate, extra-pure-grade anhydrous sodium carbonate, and extra-pure diatomaceous earth and zirconium oxide were purchased from Nacalai Tesque Co., and high-quality water with a specific resistivity of  $18 \text{ M}\Omega \cdot \text{cm}$  was filtered through a  $0.2 \mu\text{m}$  filter before use.

The experimental procedures are described briefly below. Desired quantities of water and  $\text{CaCl}_2$  solution were poured into a crystallizer and mixed by a magnetic stirrer to form a solution of specified concentration. After the solution temperature became steady at 298 K and the conductivity remained constant for several minutes, a required quantity of  $\text{Na}_2\text{CO}_3$  solution at 298 K was added into the crystallizer. The concentration of  $\text{Na}_2\text{CO}_3$  was determined by the trial-and-error method for preventing spontaneous nucleation from occurring when the two solutions were mixed. The solution conductivity, which was recorded automatically, increased rapidly to a higher level and stayed there for a certain period of time once the mixing was complete. Then, a decrease in conductivity was observed while the solution was still clear. Afterward, the solution became turbid, as detected by the naked eye, while the conductivity continued to drop. The experiment was stopped after the conductivity had no more significant change. After each run, the experimental apparatus was rinsed with 0.1 M aqueous HCl solution to remove residual precipitate. In the experiments, two same-concentration solutions of  $\text{CaCl}_2$  and  $\text{Na}_2\text{CO}_3$  were used. The investigated concentra-

**Table 3. Nucleation Rate Calculated at Different Supersaturations and Concentrations of Diatomaceous Earth**

W (mg)	1/[FP] (cm <sup>3</sup> /no.)	<i>S<sub>a</sub></i> = 4.59		<i>S<sub>a</sub></i> = 5.49		<i>S<sub>a</sub></i> = 5.85		<i>S<sub>a</sub></i> = 6.41		<i>S<sub>a</sub></i> = 6.90	
		<i>J<sub>h</sub></i> (no./cm <sup>3</sup> s)	<i>J<sub>p</sub></i> (no./cm <sup>3</sup> s)								
0	0	0.003484		0.005495		0.007576		0.011765		0.022727	
2	0.004464	0.004587	0.001103	0.006757	0.001262	0.009804	0.002228	0.014706	0.002941	0.026316	0.003589
3	0.002985	0.005000	0.001516	0.007353	0.001858	0.010870	0.003294	0.015385	0.003620	0.027778	0.005051
5	0.001789	0.005376	0.001892	0.008333	0.002838	0.012500	0.004924	0.018519	0.006754	0.031250	0.008523
8	0.001119	0.006579	0.003095	0.009524	0.004029	0.014286	0.006710	0.020833	0.009068	0.031250	0.008523
11	0.000813	0.007246	0.003762	0.010000	0.004505	0.015385	0.007809	0.020833	0.009068	0.035714	0.012987
15	0.000596	0.007692	0.004208	0.011111	0.005616	0.016667	0.009091	0.022727	0.010962	0.035714	0.012987

**Table 4. Nucleation Rate Calculated at Different Supersaturations and Concentrations of Zirconium Oxide**

W (mg)	1/[FP] (cm <sup>3</sup> /no.)	<i>S<sub>a</sub></i> = 4.59		<i>S<sub>a</sub></i> = 5.49		<i>S<sub>a</sub></i> = 5.85		<i>S<sub>a</sub></i> = 6.41		<i>S<sub>a</sub></i> = 6.90	
		<i>J<sub>h</sub></i> (no./cm <sup>3</sup> s)	<i>J<sub>p</sub></i> (no./cm <sup>3</sup> s)								
0	0	0.003484		0.005495		0.007576		0.011765		0.022727	
2	0.000754	0.003937	0.000453	0.006024	0.000529	0.008696	0.001120	0.013514	0.001749	0.024390	0.001663
3	0.000503	0.004082	0.000598	0.006250	0.000755	0.009091	0.001515	0.014706	0.002941	0.026316	0.003589
5	0.000302	0.004444	0.000960	0.006757	0.001262	0.010000	0.002424	0.016129	0.004364	0.027778	0.005051
8	0.000189	0.005000	0.001516	0.007353	0.001858	0.011111	0.003535	0.016667	0.004902	0.027778	0.005051
11	0.000137	0.005263	0.001779	0.007813	0.002318	0.012195	0.004619	0.019231	0.007466	0.029412	0.006685
15	0.000101	0.005556	0.002072	0.008333	0.002838	0.013158	0.005582	0.019231	0.007466	0.029412	0.006685

tions of CaCl<sub>2</sub> and Na<sub>2</sub>CO<sub>3</sub> solution ranged from 0.00125 M to 0.00300 M. The operating volume of solution is 200 cm<sup>3</sup>. Supersaturation was evaluated in the strict thermodynamic form as  $S_a = C_{CaCO_3} \gamma_{\pm} / C_{CaCO_3,eq} \gamma_{\pm,eq}$ , where  $C_{CaCO_3}$  is the initial concentration of CaCO<sub>3</sub>,  $C_{CaCO_3,eq}$  is the equilibrium concentration of CaCO<sub>3</sub> in an aqueous NaCl solution, which can be found in the literature,<sup>19</sup> and  $\gamma_{\pm}$  and  $\gamma_{\pm,eq}$  are the mean activity coefficient and the equilibrium mean activity coefficient, respectively, which are estimated from the Bromley correlation.<sup>20</sup>

In the case for investigating the foreign particle effect, the procedures are the same except that a desired weight of foreign particles was added into the crystallizer before the addition of aqueous Na<sub>2</sub>CO<sub>3</sub> solution. The weight of foreign particles investigated in the present work ranges from 2 to 15 mg. In all runs, the solution temperature was kept at 298 K. The concentration of foreign particles, [FP], is related to the weight of the foreign particles,  $W_{FP}$ , by the following equation:

$$[FP] = \frac{6W_{FP}}{\pi V \rho d^3} \quad (16)$$

where  $V$  is the volume of solution, and  $\rho$  and  $d$  are the density and average diameter of the particle, respectively. The values of  $\rho$  and  $d$  for the two foreign particles used in this study are 2.33 g/cm<sup>3</sup> and 33.22 μm for diatomaceous earth and 2.85 g/cm<sup>3</sup> and 17.16 μm for zirconium oxide, respectively, and are obtained experimentally by using a density meter (model SMK-401, Shimadzu) and a particle size analyzer (model LS230, Coulter), respectively.

## Results and Discussion

A typical desupersaturation curve for the mixing of 0.0020 M CaCl<sub>2</sub> and Na<sub>2</sub>CO<sub>3</sub> solution with 2 mg of diatomaceous earth as the foreign particle at 298 K is shown in Figure 1. The time interval when the conductivity of solution remains constant is defined as the induction period,  $t_{ind}$ . The induction period can be easily determined if that portion of the desupersaturation curve is enlarged as shown in the upper right corner of Figure 1, in which the solution conductivity is constant between 60 and 150 s, then suddenly drops after that. The induction

period so determined is very close to the true induction period. Therefore, the growth time can be negligible. The experimental data of the induction period obtained at various supersaturations and different weights of foreign particles are given in Table 1 for diatomaceous earth. Table 1 reveals that the induction period decreases with an increase in supersaturation for all levels of weight of foreign particles. From the nucleation theory, the foreign surfaces present in a supersaturated solution reduce the free energy required for nucleation.<sup>2</sup> Therefore, an increase in foreign particles decreases the induction period when the supersaturation is fixed. Figure 2 illustrates the induction period as a function of concentration of diatomaceous earth at five different levels of supersaturation (i.e., 4.59, 5.49, 5.85, 6.41, and 6.90). The results show that the induction period decreases with an increase in the concentrations of the foreign particles. However, no significant difference in induction period obtained at higher particle concentrations is observed, as the supersaturation is high (i.e.,  $S_a = 6.41$  and 6.90). It is known that the bulk nucleation rate is the dominant mode at high supersaturation. On the other hand, the particle-induced nucleation rate is relatively small. Therefore, the influence of foreign particles on the induction period can be neglected at high supersaturation. The experimental data of the induction period obtained at various supersaturations and different weights of the foreign particle for zirconium oxide as the foreign particle are given in Table 2. They reveal that the effects of zirconium oxide on the induction period are similar to those obtained from diatomaceous earth. In addition, the induction period obtained in the presence of zirconium oxide as the foreign particle is generally longer than those obtained from the foreign particles of diatomaceous earth at the same supersaturation of solution and weight of particles. Here, the study of Söhnel and Mullin<sup>14</sup> was employed to confirm that all nucleation in the present work was heterogeneous nucleation. The experimental data of Söhnel and Mullin were plotted by  $\log t_{ind}$  versus  $(\log S_a)^{-2}$ . The result showed that the experimental data were fitted by two straight lines of different slopes, which indicated that two different nucleation mechanisms, that is, heterogeneous nucleation at low supersaturation and homogeneous nucleation at high supersaturation, were differentiated. The data obtained in this experiment fell in the heterogeneous region.

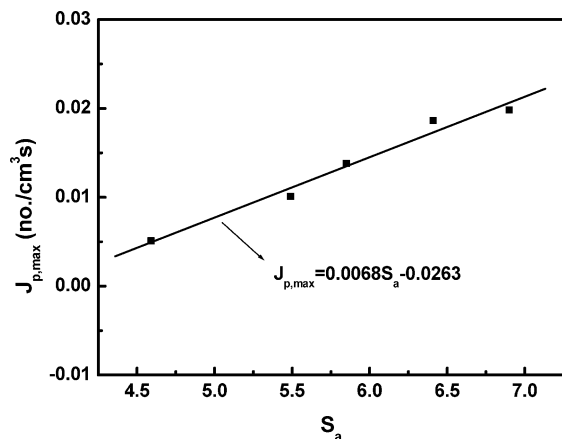


**Figure 5.**  $J_{p,\max}$  as a linear function of  $S_a$  for zirconium oxide as the foreign particle: (■) calculated points ( $J_{p,\max}$ ,  $S_a$ ).

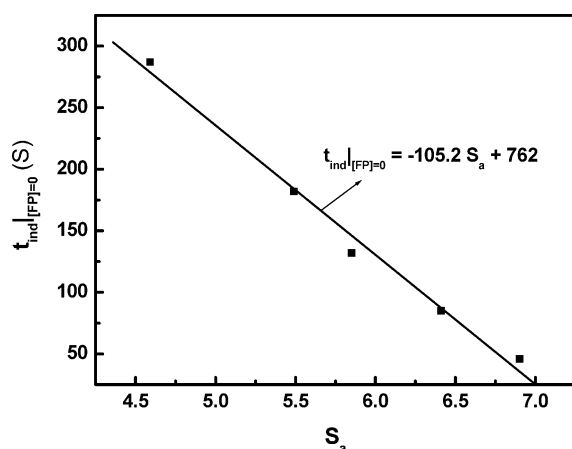


**Figure 6.** Induction period without adding foreign particles as a linear function of  $S_a$ : (■) experimental points.

Moreover, using the experimental data of the induction period listed in Tables 1 and 2, the heterogeneous nucleation rate  $J_h$  and the particle-induced nucleation rate  $J_p$  are calculated by using eq 1. The value of  $J_h$  is calculated as the reciprocal of  $t_{\text{ind}}|_{[\text{FP}] \neq 0}$ , which is the induction period obtained in the presence of added foreign particles (i.e.,  $W \neq 0$ ). On the other hand, the values of the bulk nucleation rate,  $J_b$ , as the reciprocal of  $t_{\text{ind}}|_{[\text{FP}] = 0}$  is calculated by using eq 3, which is the induction period without adding foreign particles (i.e.,  $W = 0$ ). Then,  $J_p$  can be calculated since it is the difference between  $J_h$  and  $J_b$ . The calculated  $J_h$  and  $J_p$  values at various supersaturations and different concentrations of foreign particles are given in Tables 3 and 4 for diatomaceous earth and zirconium oxide, respectively. Note that the first row in Tables 3 and 4 also represents the values of  $J_b$  because these data are obtained at  $W = 0$ . Figure 3 shows that the plot of  $1/J_p$  versus  $1/[\text{FP}]$  for the foreign particles of diatomaceous earth at  $S_a = 4.59$  gives a straight line of slope  $1.738 \times 10^5$  and intercept 146.1 with a linear correlation coefficient of 0.991. It is found that plots of  $1/J_p$  versus  $1/[\text{FP}]$  at various supersaturations give a family of straight lines of a different slope ( $K_M/J_{p,\max}$ ) and intercept ( $1/J_{p,\max}$ ). The calculated values of  $J_{p,\max}$  and  $K_M$  at five different levels of supersaturation are listed in Table 5 for the presence of diatomaceous earth and zirconium oxide. Table 5 reveals that the average values of  $K_M$  are  $1.505 \times 10^3$  no./cm<sup>3</sup> and  $1.563 \times 10^4$  no./cm<sup>3</sup> for diatomaceous earth and zirconium oxide, respectively. The values of  $K_M$  obtained at different supersaturations are close to their average value. It indicates that the

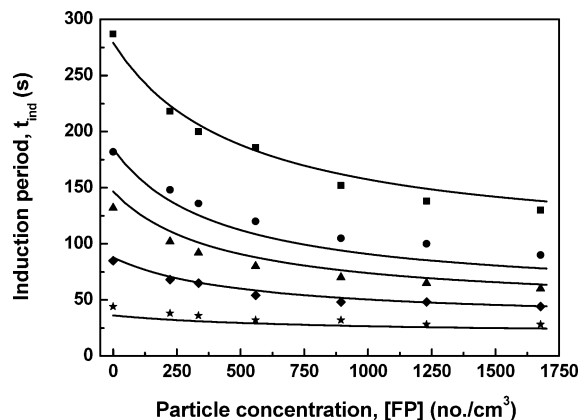


**Figure 7.** Calculated curves of induction period calculated by using eq 24 for diatomaceous earth as the foreign particle: (■) experimental points for  $S_a = 4.59$ ; (●) experimental points for  $S_a = 5.49$ ; (▲) experimental points for  $S_a = 5.85$ ; (◆) experimental points for  $S_a = 6.41$ ; (★) experimental points for  $S_a = 6.90$ .

**Table 5.** The Values of  $K_M$  and  $J_{p,\max}$  Obtained by Using the Method of a Double-Reciprocal Plot

foreign particle: diatomaceous earth					
$S_a$ (-)	$K_M/J_{p,\max}$ (s)	$1/J_{p,\max}$ (cm <sup>3</sup> s/no.)	correlation coefficient	$J_{p,\max}$ (no./cm <sup>3</sup> s)	$K_M$ (no./cm <sup>3</sup> )
4.59	$1.738 \times 10^5$	146.1	0.991	0.00684	$1.190 \times 10^3$
5.49	$1.573 \times 10^5$	80.1	0.995	0.01248	$1.964 \times 10^3$
5.85	$8.695 \times 10^4$	53.3	0.998	0.01876	$1.631 \times 10^3$
6.41	$6.806 \times 10^4$	45.9	0.986	0.02179	$1.483 \times 10^3$
6.90	$5.232 \times 10^4$	41.6	0.989	0.02404	$1.258 \times 10^3$
foreign particle: zirconium oxide					
$S_a$ (-)	$K_M/J_{p,\max}$ (s)	$1/J_{p,\max}$ (cm <sup>3</sup> s/no.)	correlation coefficient	$J_{p,\max}$ (no./cm <sup>3</sup> s)	$K_M$ (no./cm <sup>3</sup> )
4.59	$2.742 \times 10^6$	196.7	0.996	0.005084	$1.394 \times 10^4$
5.49	$2.384 \times 10^6$	99.0	0.998	0.010101	$2.408 \times 10^4$
5.85	$1.112 \times 10^6$	72.5	0.998	0.013793	$1.533 \times 10^4$
6.41	$6.499 \times 10^5$	53.7	0.986	0.018622	$1.210 \times 10^4$
6.90	$6.404 \times 10^5$	50.5	0.940	0.019802	$1.268 \times 10^4$

affinity for diatomaceous earth is greater than that for zirconium oxide. The result is quite reasonable since diatomaceous earth is a high porous material, as opposed to the dense crystalline of zirconium oxide, and thus the adsorption between the diatomaceous earth and the calcium carbonate cluster is strong. Here, we also find that the maximum particle-induced nucleation rate,  $J_{p,\max}$ , increases linearly with increasing supersaturation. Therefore, we try to express the  $J_{p,\max}$  of diatomaceous earth and zirconium oxide as a linear function of  $S_a$ , as shown in Figures 4 and 5, respectively. The linear equations and their correlation coefficient,  $R$ , can be expressed as

$$J_{p,\max} = 0.00782S_a - 0.02895, R = 0.981 \text{ for diatomaceous earth (17)}$$

and

$$J_{p,\max} = 0.00680S_a - 0.02630, R = 0.988 \text{ for zirconium oxide (18)}$$

For further simplifying the correlation of the induction period, we try again to express  $J_b$  as a function of  $S_a$ . A plot of  $t_{\text{ind}}|_{[\text{FP}] = 0}$  and  $S_a$  gives a straight line as shown in Figure 6. It indicates that the  $t_{\text{ind}}|_{[\text{FP}] = 0}$  can be expressed as a linear function of  $S_a$ :

$$t_{\text{ind}}|_{[\text{FP}] = 0} = -105.2S_a + 762 \quad (19)$$

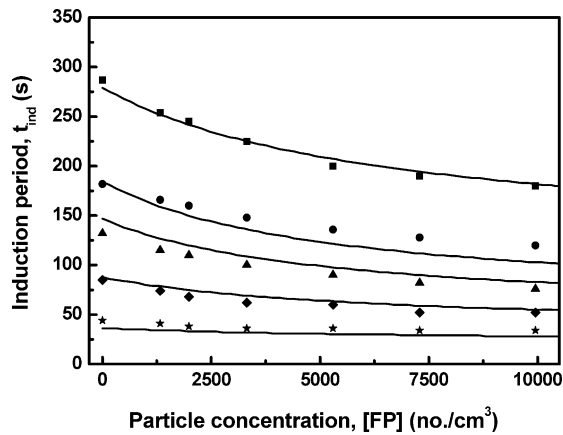


**Figure 8.** Calculated curves of the induction period calculated by using eq 25 for zirconium oxide as the foreign particle: (■) experimental points for  $S_a = 4.59$ ; (●) experimental points for  $S_a = 5.49$ ; (▲), experimental points for  $S_a = 5.85$ ; (◆) experimental points for  $S_a = 6.41$ ; (★) experimental points for  $S_a = 6.90$ .

Then eq 3, the nucleation rate occurred in the bulk of solution, may be written as the following correlation:

$$J_b = \frac{1}{t_{\text{ind}}|_{[\text{FP}] = 0}} = \frac{1}{-105.2S_a + 762} \quad (20)$$

According to eq 13, the nucleation rate originated from the surface of added foreign particles can be expressed as

$$J_p = (0.00782S_a - 0.02895) \frac{[\text{FP}]}{1.505 \times 10^3 + [\text{FP}]} \text{ for diatomaceous earth} \quad (21)$$

and

$$J_p = (0.00680S_a - 0.02630) \frac{[\text{FP}]}{1.563 \times 10^4 + [\text{FP}]} \text{ for zirconium oxide} \quad (22)$$

From eqs 20, 21, and 22, the values of  $J_b$  and  $J_p$  can be calculated by using the supersaturation of the solution and the concentration of foreign particles.

Substituting  $J_p$  and  $J_b$  into eq 2, the heterogeneous nucleation rate,  $J_h$ , can be expressed as the following correlation:

$$J_h = \frac{1}{-105.2S_a + 762} + \frac{(0.00782S_a - 0.02895)[\text{FP}]}{1.505 \times 10^3 + [\text{FP}]} \text{ for diatomaceous earth} \quad (23)$$

and

$$J_h = \frac{1}{-105.2S_a + 762} + \frac{(0.00680S_a - 0.02630)[\text{FP}]}{1.563 \times 10^4 + [\text{FP}]} \text{ for zirconium oxide} \quad (24)$$

Then, the heterogeneous induction period,  $t_{\text{ind}}|_{[\text{FP}] \neq 0}$ , can be easily calculated from the reciprocal of  $J_h$ . Comparing the reported expression of  $t_{\text{ind}}$ , which is complex and some parameters involved are difficult to determine, the present correlation is much simpler because the supersaturation of the solution and the concentration of foreign particles are easy to

measure in a crystallization system. Figures 7 and 8 illustrate the curves of the induction period calculated by using eqs 23 and 24 for diatomaceous earth and zirconium oxide, respectively. The experimental data of the induction period is also shown for comparison. The result indicates that the calculated curves are close to the experimental points. It means that the novel description based on the Michaelis–Menten equation for the heterogeneous nucleation rate of calcium carbonate was satisfactory to describe the experimental data of  $t_{\text{ind}}$ .

## Conclusion

A novel description for the  $t_{\text{ind}}$  of heterogeneous nucleation by using the Michaelis–Menten equation was proposed. In this model, the formation of nuclei was assumed to go through a series of adsorption–desorption steps between the calcium carbonate cluster and the foreign particle, and, subsequently, a surface integrated reaction took place on the foreign particle. The results showed that the obtained affinity for diatomaceous earth was greater than that for zirconium oxide. It also showed that the concentration of the foreign particle had a great influence on the  $t_{\text{ind}}$  at low supersaturation. However, the effect of foreign particles on the induction period at high supersaturation was negligible. The obtained correlations of heterogeneous nucleation rate and induction period were expressed as a function of the supersaturation of the solution and the concentration of the foreign particles. It was simpler than those reported in the literature because the supersaturation of the solution and concentration of the foreign particles are easy to measure in the studied systems. A comparison between the calculated and experimental results showed that the Michaelis–Menten equation was satisfactory to describe the experimental data of  $t_{\text{ind}}$  and to derive the nucleation rate for the heterogeneous nucleation of calcium carbonate.

## Acknowledgment

This study is supported by the National Science Council of the Republic of China.

## Literature Cited

- (1) Söhnel, O.; Garside, J. *Precipitation: Basic Principles and Industrial Applications*; Butterworth-Heinemann: Oxford, 1992.
- (2) Mullin, J. W. *Crystallization*; Butterworth-Heinemann: Oxford, 1993.
- (3) Söhnel, O.; Mullin, J. W. A Method for the Determination of Precipitation Induction Periods. *J. Cryst. Growth* **1978**, *44*, 377.
- (4) Söhnel, O.; Mullin, J. W. Precipitation of Calcium Carbonate. *J. Cryst. Growth* **1982**, *60*, 239.
- (5) Wakita, M. I. H.; Masuda, I. Analyses of Precipitation Processes of Bis(dimethylglyoximate)Ni(II) and Related Complexes. *J. Cryst. Growth* **1983**, *61*, 377.
- (6) Carosso, P. A.; Pelizzetti, E. A Stopped-Flow Technique in Fast Precipitation Kinetics – The Case of Barium Sulphate. *J. Cryst. Growth* **1984**, *68*, 532.
- (7) Kibalczyk, W.; Bondarczuk, K. Light Scattering Study of Calcium Phosphate Precipitation. *J. Cryst. Growth* **1985**, *71*, 751.
- (8) Glasner, A.; Tassa, M. The Thermal Effects of Nucleation and Crystallization of KBr Solutions. *J. Cryst. Growth* **1972**, *13/14*, 441.
- (9) Kibalczyk, W.; Zielenkiewicz, A. Calorimetric Investigations of Calcium Phosphate Precipitation. *J. Cryst. Growth* **1987**, *82*, 733.
- (10) van der Leeden, M. C.; Verdoes, D.; Kashchiev, D.; van Rosmalen, G. M. *Advances in Industrial Crystallization*; Butterworth-Heinemann: Oxford, 1991.
- (11) Gomez-Morales, J.; Torrent-Burgues, J.; Rodriguez-Clemente, R. Nucleation of Calcium Carbonate at Different Initial pH Conditions. *J. Cryst. Growth* **1996**, *169*, 331.
- (12) Joshi, M. S.; Antony, A. V. Nucleation in Supersaturated Potassium Dihydrogen Orthophosphate Solutions. *J. Cryst. Growth* **1979**, *46*, 7.
- (13) Mullin, J. W.; Záček, S. Precipitation of  $\text{KAl}(\text{SO}_4)_2 \cdot 12\text{H}_2\text{O}$  from Aqueous Solution. *J. Cryst. Growth* **1981**, *53*, 515.

- (14) Söhnel, O.; Mullin, J. W. Interpretation of Crystallization Induction Periods. *J. Colloid Interface Sci.* **1988**, 123, 43.
- (15) Nomura, T.; Alonso, M.; Kousaka, Y.; Tanaka, K. A Model for Simultaneous Homogeneous and Heterogeneous Nucleation. *J. Colloid Interface Sci.* **1998**, 203, 170.
- (16) Liu, X. Y. A New Kinetic Model for Three-Dimensional Heterogeneous Nucleation. *J. Chem. Phys.* **1999**, 111, 1628.
- (17) Bailey, J. E.; Ollis, D. F. *Biochemical Engineering Fundamentals*; McGraw-Hill: Tokyo, 1986.
- (18) Chien, W. C.; Tai, C. Y.; Hsu, J. P. The Induction Period of CaCl<sub>2</sub>-Na<sub>2</sub>CO<sub>3</sub> System: Theory and Experiment. *J. Chem. Phys.* **1999**, 111, 2657.

- (19) Linke, W. F. *Solubility, Inorganic and Metal-Organic Compounds: A Compilation of Solubility Data from the Periodical Literature*; Van Nostrand: Princeton, NJ, 1958.
- (20) Bromley, L. A. Thermodynamic Properties of Strong Electrolytes in Aqueous Solution. *AIChE J.* **1973**, 19, 313.

*Received for review* November 4, 2006  
*Revised manuscript received* April 2, 2007  
*Accepted* July 24, 2007

IE061416+